

were recorded at each trial. The distal bone fragment was also traced using the optical 3D position measurement system.

Two thresholds of software force limiter were set with respect to the developed force of the fracture model. The first threshold was set at 60N and the second threshold was set at 100N so that the robot could move freely with the reduction force of 60N, the speed of the robot slowed down inversely with an increase in the reduction force, and the robot was stopped when the reduction force reached 100N. The fracture reductions of the fracture model were reduced using the proposed methods, either with or without the software force limiter, and the movement of the bone fragment and the reduction force were compared.

B. Results

Fig. 11 shows the variations in the traction distance of the bone fragment and the reduction force during the simulated fracture reduction with and without the software force limiter. The horizontal axis is time (ms). The fracture reduction was conducted in three stages. In the first stage, the translational displacement was increased as the distal bone fragment was pulled out. As a result, the resulting force and the resulting moment were also increased. Rotation of the bone fragment was conducted during the second stage. The position and posture of the distal bone fragment was fine tuned during the third stage.

The reduction forces were always below the second threshold (100N) using the software force limiter, while the reduction forces were above this value without the software force limiter.

Fig. 12 shows the “before” and “after” status of the fracture model. The average time for the fracture reduction was 82.5s, and the difference from the normal value of the mechanical axis is shown in Table II.

V. DISCUSSION AND CONCLUSION

Simulated fracture reduction was conducted using the RCC-PA mode of the fracture-reduction robot. A software force limiter using two threshold levels can prevent excessive

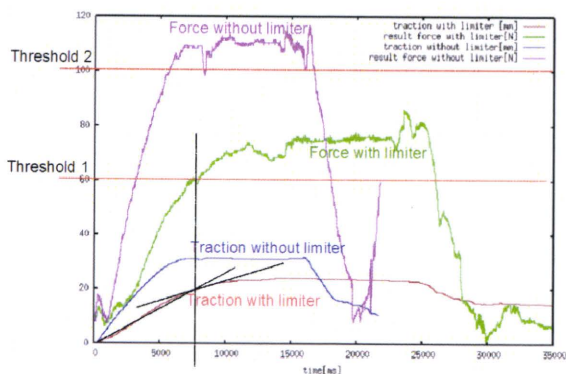
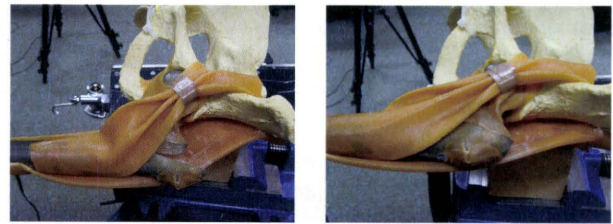


Fig. 11. Variations in traction distance and reduction force during simulated fracture reduction



(a) (b)

Fig. 12. Results of fracture reduction using the RCC-PA method: (a) before reduction and (b) after reduction.

TABLE II

FRACTURE-REDUCTION RESULTS WITH RCC-PA. () IS THE DIFFERENCE BETWEEN THE NORMAL VALUE AND THE REDUCTION VALUE

Parameter	Normal	Reduction value		
		ave	min	max
PFA, °	88.14	87.81(0.79)	86.84(0.32)	89.28(1.30)
DFA, °	90.60	90.89(0.34)	90.45(0.04)	91.34(0.74)
MA, mm	426.78	427.76(1.06)	426.44(0.26)	428.88(2.10)

force during simulated fracture reduction. Two threshold levels were set for the resultant force produced by the fracture model. The reduction force was 100N when the distal bone fragment was under traction up to 30mm, which is in the range that is safe from over-traction. Thus, the second threshold was set at 100N to avoid over-traction of the distal bone fragment. The first threshold was set at 60N, and provides information on proximity to the second threshold by a reduction in robot speed. The RCC-PA mode with the software force limiter function can reduce the fracture model without affecting the reduction motion of the robot while the reduction forces are within the second threshold. Feeling timing of the speed reduction was not evaluated. Further, this varies among different individuals. The first threshold and the speed gain slope should be modified from these data.

Threshold values must be validated using clinical data. Maeda et al. reported some reduction force clinical data [9]. However, the data were obtained from healthy subjects, using an indirect reduction method. Although these data should be considered to determine the threshold, they cannot be used to determine the threshold. Additional clinical data are required; this is an ongoing project.

A fracture-reduction procedure is generally considered accurate and precise when the alignment error and the gap are within 2° and 2mm, respectively, according to assessments based on 2D imagery. The average differences in PFA, DFA, and MA after fracture reduction using the RCC-PA mode were 0.79°, 0.34°, and 1.06mm, respectively (n=8). Although there are no recommended values for the evaluation methods used in this paper, it is believed that differences are allowable when comparing the 2D recommended values, and that the RCC-PA mode has the potential to reduce fractures with high precision.

The robot can be controlled intuitively, which means that the operators can move the bone fragment easily in the

intended manner. A surgeon who used the RCC-PA mode commented as follows:

- It was good that the fracture could be reduced using a small force.
- By constraining the rotation center, the fracture could be reduced easily and intuitively.
- The method should be evaluated using the fracture model with a rough fracture surface.

All trials were conducted under open conditions. In a clinical situation, the operator has to depend on the navigation system or fluoroscope to confirm the status of the fracture site. Therefore, the RCC-PA mode should also be evaluated in a blind situation.

We have presented safety controls for systems for assisting fracture reduction. A simulated fracture reduction was conducted using the RCC-PA mode with a software force limiter. The fracture model used in the evaluation produces reaction forces, and the accuracy of the RCC motion under the effect of the load was also evaluated. A software force limiter with two threshold levels could successfully mitigate excessive reduction. Although the results show the potential to reduce fractures with high precision, additional safety features should be developed and evaluated for clinical use of the developed system.

VI. ACKNOWLEDGMENTS

The authors thank THK CO., LTD. (JAPAN) for providing technical support to the fracture-reduction robot; Mr. Hongho Kim (Dept. Precision Engineering, the University of Tokyo) for his skilled illustration. This work was supported by Health Labour Sciences Research Grant.

REFERENCES

- [1] Cooper, C., Campion, G., and Melton, L. J., "Hip fractures in the elderly: A world-wide projection", *Osteoporosis International*, vol. 2, 1992, pp. 285-289.
- [2] M. J. PARKER and C.E. TAGG, "Internal fixation of intracapsular fractures", *Journal of the Royal College of Surgeons of Edinburgh*, vol. 47, 2002, pp. 514-547.
- [3] L.P.Müller, J.Suffner, K.Wenda, W.Mohr, and P.M.Rommens, "Radiation exposure to the hands and the thyroid of the surgeon during intramedullary nailing", *Injury*, vol. 29, 1998, pp. 461-468.
- [4] Bernd Füchtmeier, Stefan Egersdoerfer, Ronny Mai, Rainer Hente, Daniel Dragoi, Gareth Monkman, and Michael Nerlich, "Reduction of femoral shaft fractures in vitro by a new developed reduction robot system 'RepoRobo'", *Injury*, vol. 35, 2004, pp. 113-119.
- [5] Ralf Westphal, Simon Winkelbach, Friedrich Wahl, Thomas Gösling, Markus Oszwald, Tobias Hüfner, and Christian Krettek, "Robot Assisted Long Bone Fracture Reduction", *Int J of Robotics Research*, Vol. 28, 2009, pp.1259-1278.
- [6] M.Mitsuishi, N.Sugita, S.Warisawa, T.Ishizuka, T.Nakazawa, N.Sugano, K.Yonenobu, and I.Sakuma, "Development of a computer-integrated femoral head fracture reduction system", *In Proceedings of ICM '05.*, 2005, pp. 834-839.
- [7] Sanghyun Jung, Hirokazu Kamon, Hongen Liao, Junichiro Iwaki, Touji Nakazawa, Mamoru Mitsuishi, Yoshikazu Nakajima, Tsuyoshi Koyama, Nobuhiko Sugano, Yuki Maeda, Masahiko Bessho, Satoru Ohashi, Takuya Matsumoto, Isao Ohnishi, and Ichiro Sakuma, "A Robot Assisted Hip Fracture Reduction with a Navigation System", *In Proceedings of MICCAI 2008*, 2008, pp. 501-508.
- [8] S. Warisawa, T. Ishizuka, M. Mitsuishi, N. Sugano, K. Yonenobu, and T. Nakazawa, "Development of a femur fracture reduction robot", *In Proceedings of ICRA 2004*, vol. 4, 2004, pp. 3999-4004.
- [9] Y. Maeda, N. Sugano, M. Saito, K. Yonenobu, I. Sakuma, Y. Nakajima, S. Warisawa, and M. Mitsuishi, "Robot-assisted femoral fracture reduction: Preliminary study in patients and healthy volunteers", *Computer Aided Surgery*, vol. 13, 2008, pp. 148-156.
- [10] Y. Nakajima, T. Tashiro, N. Sugano, K. Yonenobu, T. Koyama, Y. Maeda, Y. Tamura, M. Saito, S. Tamura, M. Mitsuishi, N. Sugita, I. Sakuma, T. Ochi, and Y. Matsumoto, "Fluoroscopic bone fragment tracking for surgical navigation in femur fracture reduction by incorporating optical tracking of hip joint rotation center", *IEEE Transactions on Biomedical Engineering*, vol. 54, 2007, pp. 1703-1706.
- [11] Paley D., *Principles of deformity correction*, Berlin: Springer, 2001.

Effects of femur shaft fracture type on robotic assisted fracture reduction

JOUNG S¹, DOKE T², KOBAYASHI E¹, NAKAJIMA Y², SUGANO N³, BESSHO M⁴, OHNISHI I⁴, SAKUMA I¹

¹*Department of Precision Engineering, The University of Tokyo, Tokyo, Japan*

²*Department of Bioengineering, The University of Tokyo, Tokyo, Japan*

³*Graduate School of Medicine, Osaka University, Japan*

⁴*Graduate School of Medicine, The University of Tokyo Hospital, Japan*

⁵*Department of Precision Engineering, The University of Tokyo, Tokyo, Japan*

shjyoung@bmpe.t.u-tokyo.ac.jp

Introduction: Robot assisted fracture reduction has possibility to improve the reduction accuracy and the safety and to provide the convenient methods in long bone fracture reduction. Two groups have tried to use an industrial robot for fracture-reduction [1, 2]. Graham et al. introduced the parallel robot for long bone fracture reduction [3]. Our group has developed a fracture reduction assisting robotic system for hip fracture [4]. Though several studies reported robotic assisted fracture reductions, only a few reduction results were presented. Westphal et al. showed good resultants using the telemanipulated approach in the oblique fracture reduction of femur shaft [2]. Our previous studies also show good resultants with both a power assisted reduction and an automated reduction. However, no one has tried the robot assisted reduction of the spiral fracture, which is occurred by a twisting force. The goal of this study is to evaluate effects of the fracture types in the robotic assisted fracture reduction of the femur shaft fracture. We prepared two fracture types of femur shaft; an oblique and a spiral, and tried to reduce the fracture with a power assist mode and an automation mode of the fracture-reduction system. The resultants were statistically compared and the influences of fracture types were discussed.

Materials & Methods: The fracture-reduction assisting robotic system consists of the fracture-reduction robot and the navigation system. The fracture-reduction robot has six DOFs (i.e., three DOFs in translation and three DOFs in rotation). The system has two control modes; one is the power assist mode and another is the automation mode with the navigation system. The robot of which end effector is directly fixed to a distal bone fragment augments a surgeon's

force to generate enough power required for fracture reduction with the power assist mode. As the inputted forces and moments by operator, the fracture-reduction robot moves the relevant axes of the robot by centering on the bone coordinate; an operator can pull out the bone fragment according its longitudinal direction or can rotate it centering on one point that is set at a center of fracture surface. We abbreviated this control "RCC-PA" (Rotation Center Constrained Power Assistant). In case of the automated reduction, the fracture-reduction robot replaces the bone fragment based on the reduction path generated by the navigation system.

We prepared two types of femur-shaft fracture that were a simple oblique fracture and a simple spiral fracture by cutting polyurethane femur models (Composite Femur; Pacific Research Laboratories, Inc., USA) as shown in Figure 1 (a). Both fracture angles were 45° . The femoral head of the proximal fragment was connected to a pelvic model with rubber bands. And the distal fragment was fixed to the fracture-reduction robot.

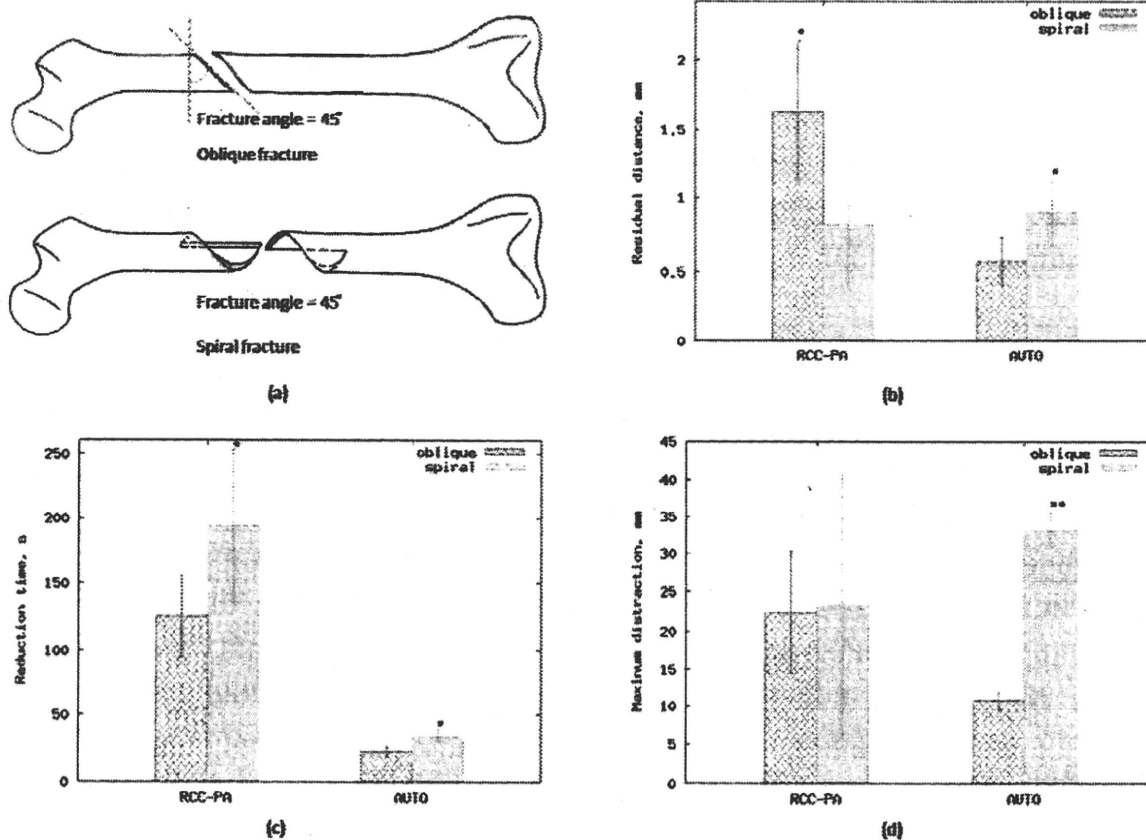


Figure 1. Fracture types and Comparisons of reduction results; (a) two fracture types of femur shaft, (b) residual distance, (c) reduction time, and (d) maximum distraction, *significant difference ($p < 0.05$) on t-test, **significant difference ($p < 0.001$) at (b), (c), and (d).

Two experimenters tried to reduce the both fracture models twice and three times respectively using RCC-PA mode only depending on the information of the navigation system, which provides the three dimensional images of the proximal and distal bone fragments and the numerical differences of distance

and angles between two coordinate of bone fragments. In experimental setup, we used the points based registration to trace the bone fragments. Five automated reductions were also conducted to both fracture models with the manually generated reduction paths.

We recorded the residual distance, angles, reduction time, and the maximum distraction after each trial and compared the resultants by student's t-test in order to know whether the fracture types influence the fracture resultants or not on two control modes. The residual distance means distance between two origin of the distal and proximal coordinate and the residual angles are between paired axes of two coordinates.

Results: *Residual distance:* Residual distances after the fracture reduction were shown in Figure 1 (b). While the residual distance of the oblique fracture is significantly larger than one of the spiral fracture with the RCC-PA mode ($p < 0.05$), residual distance is significantly smaller in the oblique fracture than in the spiral fracture with the automation mode ($p < 0.05$).

Residual angles: There are no significant differences between two fracture type, and average residual angles were smaller than 0.50 degree in RCC-PA mode and were smaller than 0.05mm in the automation reduction.

Reduction time: As shown in Figure 1 (c), reduction times significantly increased in the spiral fracture than in the oblique fracture with both two control modes ($p < 0.05$).

Maximum distraction: The mean of maximum distractions were shown in Figure 1 (d). The maximum distraction was significantly higher in the spiral fracture than in the oblique fracture with the automation mode ($p < 0.001$). However, there was no difference between two fracture types with the RCC-PA mode.

Discussion: We have developed the fracture-reduction assisting robotic system for lower limb fractures. The system has two control modes; the power assist reduction with RCC-PA control and the automation mode with the navigation system. We tried to reduce two types of fracture models-oblique and spinal-with two control modes and evaluated influences of them on reduction resultants.

During the fine alignment, bone fragments were spatially interfered with each other in spite of non-contact on the navigation system. Therefore, we consider the cause of statistical differences of residual distances as the registration error rather than characteristics of fracture types. More reduction time was required in the spiral fracture with both control methods. Especially, fine alignments of the spiral fracture were time-consuming procedure. The reduction paths of

spiral fracture were generated to prohibit the spatial interference between two bone fragments, which may deteriorates accuracy and efficiency of reduction procedures. Thus, the maximum distractions of the spiral fracture were much larger than that of the oblique fracture with the automation mode. Finding of the optimized reduction path is our challenging work. In this study, we did not compare reduction resultants between two control modes. It seems to be more acceptable that we compare these results with the resultants by a manual fracture reduction which does not use the robot or by the conventional reduction methods and this is our ongoing works.

awake during surgery and motor and language function was mapped using standard cortical electrostimulation at 5 mm intervals. During LDI acquisition, a stimulation protocol for fingertapping was performed using a visual cue. Nine fingertapping periods were performed during 8 minutes.

In Fig. 1, we show the conventional optical image of the field-of-view together with the region (black circle) that was located using presurgical fMRI for a similar fingertapping task. The statistical parametric map using GLM analysis is shown on the right side.

In Fig. 2, we depict a selection of ICA maps and time-courses after temporal sorting. Maps 1 and 2 have associated time-courses that are highly correlated to the response function, with very high statistical significance. Interestingly, these maps show a slightly different brain region. Close inspection of the respective time-courses reveals that map 2 is almost exclusively activated for the 7th fingertapping period and this activated area remains inactive for map 1. This suggests that the patient might have performed a slightly different task (e.g. different finger).

The remaining maps are not strongly related to the stimulation paradigm. Map 12 shows the complete exposed cortical surface and the associated time-course is very oscillatory, suggesting a (widespread) physiological component. Many maps capture acquisition artifacts, such as map 18 for some surface reflections. Some other maps also contain stripe artifacts, such as those in the upper part of the map “detected” by standard GLM analysis. The ability of ICA to identify nuisance components is very useful and has been reported before for other modalities such as EEG and fMRI.

Conclusion

The combination of ICA with GLM analysis can be advantageous for analysis of LDI perfusion data. Indeed, many signal components in this modality are (too) unpredictable and can hamper GLM-only analysis. On the other hand, ICA can eliminate nuisance components while at the same time identifying components that are consistent with the stimulation. Moreover, the method is computationally attractive (a couple of seconds for the 8-minutes dataset here) and repeated application of the ICA algorithm rendered almost identical maps.

The use of LDI in the operating theatre may assist the neurosurgeon and considerably shorten the time for mapping the exposed brain. It can also be used with more complex stimulation paradigms without the risk of inducing seizures. There is also a direct correspondence between the current brain position and the view of the surgeon through the surgical microscope ocular.

The observations were carried out with the approval of the ethics committee of the University Clinics of Frankfurt am Main and with the patient’s written informed consent.

User interface for decision of intended movement and its application to fracture-reduction assisting robotic system

S. Joung¹, H. Liao¹, E. Kobayashi¹, Y. Nakajima², M. Mitsuishi², N. Sugano³, I. Ohnishi⁴, I. Sakuma¹

¹The University of Tokyo, Dept. of Precision Engineering, Tokyo, Japan

²The University of Tokyo, Dept. of Bioengineering, Tokyo, Japan

³Osaka University, Graduate School of Medicine, Osaka, Japan.

⁴The University of Tokyo Hospital, Graduate School of Medicine, Tokyo, Japan

Keywords Fracture reduction robot · User interface · Femur shaft fracture

Purpose

Fracture reduction of the lower limb is burden work due to the weight of the limb and the soft tissues around the femur, and requires operator highly qualified skill and experience to figure out three

dimensional positions of bone fragments seeing only two dimensional fluoroscopic images. In order to overcome these issues, we have developed a fracture-reduction assisting robotic system for hip fracture and have already reported the navigation based control of the system [1]. Another application of the system is a power assistance mode of an orthopedic surgeon where the robot augmented the surgeon’s force to generate enough power required for fracture reduction. We installed a force/moment sensor for estimating the operator’s intended moving direction; forces are considered translational movements and moments are considered rotational movements. Because forces and moments are always acted on the same time, it is difficult to separate the translation and rotation motions from them. However our medical staffs preferred to separate the translation and rotation movement of bone for more precise reduction. Though menus on a touch panel are prepared for this purpose, it requires one more medical staff because an operator does not want to touch the panel or cannot touch it from concerns of infection.

We are planning to conduct clinical test of our system. So we select a femur shaft fracture as the first clinical application because it has more simple anatomical structure than that of a hip fracture. The purpose of the study is proposal of new interface to decide operator’s intention of motion direction based on force/torque sensor data, implementation of the proposed method in the actual fracture-reduction robot, and quantitative evaluation of the reduction accuracy utilizing proposed intention estimation algorithm.

Methods

System configuration

The fracture-reduction assisting robotic system consists of the fracture-reduction robot and the navigation system. Structure of the fracture-reduction robot is provided in Fig. 1(a); a kinematic model and the coordinate of the robot are provided in Fig. 1(b). The fracture-reduction robot has six DOFs (i.e., three DOFs in translation and three DOFs in rotation). The fracture-reduction robot has three interface devices; a touch panel, a foot switch, and a force/moment sensors installed handle. The touch panel provides menus for selecting a control mode of the robot and submenus about each control mode. A surgeon should push a foot switch during operating the fracture-reduction robot with a power assist mode. The handle, whose function is similar to a joystick, is prepared to manipulate the fracture-reduction robot.

Control methods and User interface for decision of intended movement

As the inputted forces and moments by operator, the fracture-reduction robot moves the relevant axes of the robot by centering on the bone coordinate with the proposed control method. The origin of the bone coordinates is on the center of the fracture surface and its primary axis aligns with the longitudinal direction of the bone fragment. Surgeons can track the bone fragment according its longitudinal direction or can rotate the bone fragment

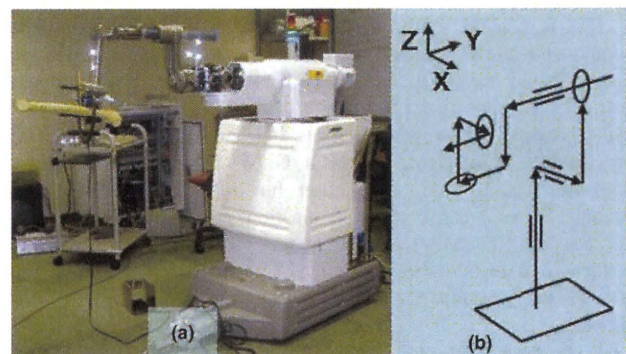
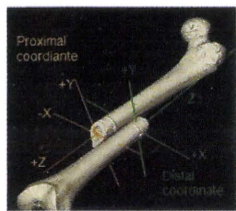


Fig. 1 The fracture reduction robot; (a): Structure of the fracture-reduction robot, (b): a kinematic model and a coordinate of the robot



	Touch panel	DIM interface
Residual distance	1.7 ± 0.75	1.1 ± 0.03
Residual angle x-axis	0.1 ± 0.04	0.4 ± 0.31
Residual angle y-axis	0.5 ± 0.32	0.6 ± 0.32
Residual angle z-axis	0.3 ± 0.33	0.3 ± 0.27
Reduction time	208 ± 70.6	340 ± 128.7

Fig. 2 The bone coordinates and the mean results after fracture reduction using two interfaces; touch panel and the DIM interface

centering on one point. This control method is called a RCC-PA (Rotation Center Constrained Power Assistant) here. We focused on the foot switch in order to decide the intended moving direction of the bone during the use of RCC-PA mode. We defined input methods of the foot switch; one push and double pushes. In our definition, the double pushes means one short push and additional push within 700 milliseconds. An operator can freely move three translation directions during one push and he can move one selected rotational direction, which is the biggest direction among the applied moments, during double pushes. We will note this interface to DIM (Decision of Intended Movement) interface at left of this abstract.

Fracture reduction evaluation

We prepared a model of femur-shaft fracture that is simple oblique fracture (fracture angle > 30°) by cutting a polyurethane femur model. The femoral head of the proximal fragment was connected to a pelvic model with rubber bands. And the distal fragment was fixed to the fracture-reduction robot.

We used the points based registration to trace the coordinate of the distal and proximal bone fragments. Three stainless-steel screws were inserted each bone fragment before CT scan. The real positions of the screws were localized with a pen-type reference marker and an optical motion capture system (Optotrak Certus; NDI, Canada). Five orthopedic surgeons tried to reduce the fracture using RCC-PA mode by once with two user interfaces; the touch panel and DIM interface. While surgeons reduced the fracture, the fracture region was blinded and they could only depend on the information of the navigation system, which provides the three dimensional images of the proximal and distal bone fragments and the numerical differences of distance and angles between two coordinate of bone fragments. We compared two reduction resultants by student's t-test. The hypothesis was that the residual distance, the angles, and the reduction time did not differ between two interfaces. Statistical significance was set at $p < 0.05$. The residual distance was defined as distance between two origin of the distal and proximal coordinate and the residual angles were defined as the angles between paired axes of two coordinates.

Results

The coordinates of the bone fragments and the mean of the residual distance, the residual angles, and the reduction time are presented in Fig. 2. There are no differences in the resultants between two interfaces. In the fracture reduction with the proposed interface, the reduction procedure was deactivated once because of the large movement of the proximal bone fragment occurred by a contact between two bone fragments. We should reposition the proximal bone because of the excess of the robot's operational range.

Conclusion

We have developed the fracture-reduction assisting robotic system for fractures of lower limb. In this paper, we introduced the user interface to decide the intended moving direction of the bone fragment with the fracture-reduction robot. And we compared the reduction resultants by two interfaces; one is the use of buttons on the touch panel and another is DIM interface, which uses a foot switch and the magnitude of the moments. There are no differences between reduction results.

Surgeons all degreed that they did not feel the inconvenience for double pushes and could rotate the bone to direction that they wanted to move without an assistant. For clinical use of our system, the additional studies about safety and fracture types will be evaluated with the improved and various fracture models.

Acknowledgements

The authors thank orthopedic surgeons of the University of Tokyo Hospital for their cooperation and help in this study. This work was supported by Health Labour Sciences Research Grant.

Reference

- [1] Sanghyun Jung, Hirokazu Kamon, Hongen Liao, Junichiro Iwaki, Touji Nakazawa, Mamoru Mitsuishi, Yoshikazu Nakajima, Tsuyoshi Koyama, Nobuhiko Sugano, Yuki Maeda, Masahiko Bessho, Satoru Ohashi, Takuya Matsumoto, Isao Ohnishi, and Ichiro Sakuma, "A Robot Assisted Hip Fracture Reduction with a Navigation System", In Proceedings of MICCAI 2008, 2008, pp. 501–508.

Analysis of the micro-migration of sliding hip screws by using point-based registration

P. Raudaschl, K. Fritscher, T. Roth, Ch. Kammerlander, R. Schubert University for Health Informatics and Technology Tyrol, Institute for Biomedical Image Analysis, Hall, Austria

Keywords Hip fractures · Sliding hip screw · Micro-migration · Cutout

Purpose

Nowadays the sliding hip screw is the favored treatment method for hip fractures, and its usage will increase in the future, especially due to the growing number of elderly people. Hence, it is important that the number of implant failures will be reduced and that complications can be detected earlier. The most frequently occurring failure is the cutout of the screw from the femoral head. This happens particularly if the patient is older and/or suffers from osteoporosis. Consequently, the screw should be implanted at the best possible position, so that fixation is ideal for the individual patient. There are a lot of different studies which have tried to find parameters like screw position [1], bone quality, fracture pattern [2], patient age or tip-apex distance [3] to identify this type of failure of fixation.

In this work we propose a method for the early diagnosis of a possible cutout by evaluation of micro-migration of the screw in the femoral head by using CT images.

Methods

A tool which enables the quantification of the micro-migration of the screw out of CT images that were acquired at two different time points (post-OP and 3-month-control check up CTs) was developed.

In order to evaluate micro-migration using CT images, it is necessary to align the two images using image registration methods. Hence, before performing registration and transformation, the following preprocessing steps were necessary:

- segmentation of the screw through thresholding
- clipping the front part of the screw
- creating point sets for the following image processing

After these preprocessing steps, the ICP algorithm [4], which aims at iteratively finding the optimal transformation from the fixed point set (represents post-OP image) to the moving point set (represents 3-month-control image), was applied. The resulting transformation matrix was used to align the 3-month-control image. The accuracy of the registration was evaluated by using the mean Euclidian metric.

In order to assess the micro-migration of the screw, the following method was used: The largest possible sphere in the femoral head was placed in both images, post-OP and 3-month-control CT. The overall

0806 Universal-Bar-Link 創外固定器の位置姿勢誘導システムの開発 Development of navigation system for Universal- Bar-Link external fixator

○学 石原良太 (東京大学), 鄭常賢 (東京大学), 小林英津子 (東京大学), 大西五三男 (東京大学), 佐久間一郎 (東京大学)
R.Ishihara,the University of Tokyo,S.Joung, the University of Tokyo, E.Kobayashi, the University of Tokyo,I.Ohnishi, the University of Tokyo,I.Sakuma the University of Tokyo

Keywords: deformed bone, Universal-Bar-Link external fixator, navigation system

1. 背景

本研究では変形骨整復のために東京大学医学部整形外科-大西らを中心に開発された Universal-Bar-Link 創外固定器 (以下 UBL 創外固定器) を用いる^[1]。変形骨に対して正確な位置と姿勢に UBL 創外固定器を設置する必要があるが、現状では正確な設置が困難である。そのためナビゲーションシステムが非常に有用である。ナビゲーションシステムは X 線 CT・光学式 3 次元位置計測装置 (Polaris, Northern Digital Inc.社 以下ポラリス)・手動位置姿勢決め装置から構成される。ナビゲーションシステム全体の要求精度は近位部クランプの Position 誤差 5[mm],Posture 誤差 5[degree]であり、手動位置姿勢決め装置単体の要求精度は Position 誤差 2[mm],Posture 誤差 2[degree]である^[2]。手動位置姿勢決め装置は、位置制御を行う空気圧駆動把持アーム (ポイントセッター、三鷹光器社以下ポイントセッター) と姿勢制御を行う骨接合材料姿勢制御器具からなる。先行研究では位置・姿勢の誤差が大きい点が問題となっていた。この原因の第一として器具の剛性の低さが挙げられる。骨接合材料姿勢制御器具の改良および位置誘導評価実験を行ったので報告する。

2. 骨接合材料姿勢制御器具の改良

前試作機に対して、材質の変更・構造の変更・使用するエンコーダの変更を行うことでより頑強で軽量化された骨接合材料姿勢制御器具を開発した。また、ポイントセッターと骨接合材料姿勢制御器具の連結部に X-Y-Z 微動調整機構を取り付けることで、位置誘導の操作性と精度の向上を図った。前試作機では LED ユーザインタフェースを使用していたが、4.3inch の小型ディスプレイをポイントセッター手元に取り付けることで術者の操作性向上を図った。(Fig.1)

3. 位置誘導評価実験

新しく採用した X-Y-Z 微動調整機構および小型ディスプレイによる操作性・精度の評価のために位置誘導評価実験を行った。手動位置姿勢決め装置を適当な初期位置に置いた状態で、設定した目標位置まで位置誘導するのにかかる時

間と目標位置までの距離誤差を計測した。試行回数 10 回を行い、誘導時間は平均 71[sec]・位置誤差は平均 0.1[mm]となった。

4. 考察

位置誘導にかかる時間は 71[sec]と大変短くなっており、術者・患者にかかる負担の軽減につながると考えられる。位置誤差平均 0.1[mm]は手動位置姿勢決め装置の要求精度 2[mm]に比べて非常に小さい。

5. 今後の予定

依然として姿勢制御器具の剛性が低いので剛性向上を図る。また、模擬骨に対して新しく開発した器具でナビゲーションを行い精度の評価を行う。

謝辞

本研究の一部は厚生労働科学研究費補助金による。

文献

- [1]大西五三男 他：ユニバーサル・バー・リンク・機構を有する片側式創外固定器による変形矯正、日本創外固定・骨延長学会雑誌、18
- [2]池邊賢治：Universal-Bar-Link 創外固定器を用いた骨折整復のためのナビゲーション開発、16回日本コンピュータ外科学会誌、pp.175-176、2007Page53-61(2007)

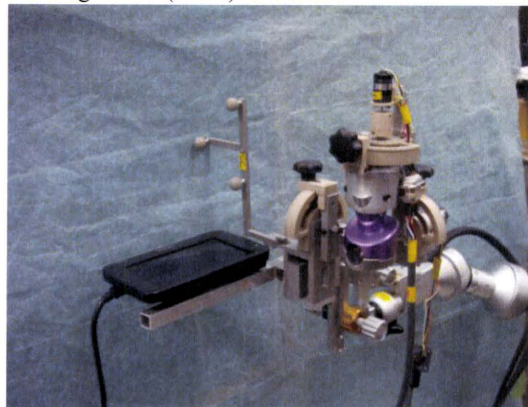


Fig.1 New osteosynthesis materials posture control apparatus

